

Controlled growth of silicon nanowires on silicon surfaces

Billel Salhi · Bruno Grandidier · Rabah Boukherroub

Received: January 21, 2005 / Revised: April 23, 2005 / Accepted: May 25, 2005
© Springer Science + Business Media, Inc. 2006

Abstract This paper reports on silicon nanowire growth on oxidized silicon substrates using different approaches for gold catalyst deposition. The gold coated surfaces and the resulting nanowires were characterized using scanning electron microscopy. The gold catalysts were made up of gold nanoparticles (50 nm diameter), which were either dispersed or spotted at different concentrations using a robot, or were formed on a patterned Si/SiO₂ substrate by metal evaporation (63 nm diameter). The subsequent silicon nanowire growth was accomplished by CVD decomposition of silane gas (SiH₄) at high temperature (400–500°C) in a vapor-liquid-solid (VLS) process. Under these conditions, a high density of silicon nanowires (SiNWs) was achieved on the oxidized silicon surfaces, but the distribution of the nanowires was found to be inhomogeneous in the case of the gold nanoparticles. Such result is attributed to the aggregation of the nanoparticles during the growth process. Alternatively, when gold nanodot catalysts were lithographically patterned on the surface, the nanowires were obtained in the patterned regions.

Keywords Gold nanoparticles · Silicon nanowires · Vapor-liquid-solid process · E-beam lithography · Scanning electron microscopy

B. Salhi · R. Boukherroub (✉)
Interdisciplinary Research Institute (IRI)
Institut d'Electronique de Microélectronique et de
Nanotechnologie, UMR CNRS-8520, Cité Scientifique, Avenue
Poincaré - BP. 60069, 59652 Villeneuve d'Ascq, France
e-mail: rabah.boukherroub@iemn.univ-lille1.fr

B. Grandidier
Institut d'Electronique de Microélectronique et de
Nanotechnologie, UMR CNRS-8520, Cité Scientifique, Avenue
Poincaré - BP. 69, 59652 Villeneuve d'Ascq, France

Introduction

Semiconductor nanowires have attracted great attention owing to their submicron ultimate feature size, to the expected original electrical and optical properties and the potential applications in the field of nanoelectronics, high-speed field effect transistors, bio and chemical sensors, and light-emitting devices with low power consumption [1–8]. Silicon nanowires (SiNWs) are of special interest, because silicon is the basic material in microelectronics. The big demand for building powerful devices and the limits of the present approaches based on lithographic techniques to achieve few nanometer size components require the development of new methods. Control of the synthesis and the surface properties of SiNWs may open new opportunities in the field of silicon nanoelectronics and use the SiNWs as nanocomponents to build nano circuits and nanobiosensors.

Diverse methods have been used to prepare Si nanowires (SiNWs). Silicon nanowires have been synthesized by laser ablation of metal-containing silicon targets [9–11]. SiNWs have also been prepared by an “oxide-assisted” technique, which consists on thermal evaporation of highly pure powder mixture of silicon and silicon dioxide at 1200°C. However, the nanowires obtained by this method display a high density of defects, a broad diameter distribution, and a thick oxide shell [12]. Many of the SiNWs investigations regarding their synthesis have employed the so-called Vapor-Liquid-Solid (VLS) process proposed by Wagner in 1960s during his studies of large single crystalline whisker growth [13, 14]. The fundamental process is based on metal catalyst directed chemical vapor deposition of silicon. According to this mechanism, the anisotropic crystal growth is promoted by the presence of liquid alloy/solid interface. This technique is carried out in the presence of gold or other metal nanoparticles catalysts at high temperature. Based on Si-Au binary

phase diagram, Si (from the decomposition of SiH_4) and Au form a liquid alloy when the temperature is higher than the eutectic point (363°C). The liquid surface has a large accommodation coefficient and is therefore a preferred deposition site for incoming Si vapor. After the liquid alloy becomes supersaturated with Si, Si nanowire growth occurs by precipitation at the solid-liquid interface. In principle, the diameter, the length, the composition and the electronic properties of SiNWs can be controlled during the synthesis. The VLS technique was applied by several groups for the synthesis of SiNWs in a controlled fashion [15, 16]. In this process, the diameter of the nanowires is determined by the diameter of the catalyst particles and therefore, the method provides an efficient means to obtain uniform-sized nanowires. SiNWs with a narrow size distribution were obtained by using well-defined catalysts (gold nanoparticles).

It was possible to tune the electronic properties of the nanowires by including doping precursors in the silane gas. Boron and phosphorus-doped silicon nanowires were obtained this way [17–19]. Controlling the growth orientation is important for the applications of nanowires. Nanowires generally have preferred growth directions. For example, silicon nanowires grow along the $\langle 111 \rangle$ direction when grown by the VLS process, but can be made to grow along the $\langle 112 \rangle$ or the $\langle 110 \rangle$ direction by the oxide-assisted growth mechanism. These results demonstrate a clear preference for growth along the $\langle 110 \rangle$ direction in the smallest SiNWs and along the $\langle 111 \rangle$ direction in larger SiNWs [19].

Direct evidence for germanium nanowire growth mechanism in a VLS process has unambiguously been confirmed by conducting real-time in situ transmission electron microscopy (TEM) studies at high temperature [20]. The experiment result clearly shows three growth stages: formation of Au-Ge alloy, nucleation of Ge nanocrystal and elongation of Ge nanowire. This observation demonstrates the validity of the VLS mechanism for nanowire growth. The establishment of VLS mechanism at the nanometre scale is very important for the rational control of inorganic nanowires, since it provides the necessary underpinning for the prediction of metal solvents and preparation conditions.

A solution phase for silicon nanowires preparation with diameter size less than 10 nm and a narrow size distribution using fluid-liquid-solid (FLS) method was proposed in the literature. In this solution phase process, a precursor such as diphenylsilane was thermally degraded in supercritical fluid at 400 to 500°C in the presence of gold nanocrystals [21–23]. Using this technique, single crystal SiNWs were synthesized, although the surfaces may be contaminated by hydrocarbon.

In this paper, we report on our results on the synthesis of SiNWs with well-controlled diameter by using well defined Au nanoclusters catalysts and silane (SiH_4) as the vapor phase reactant. In the first stage, 50 nm diameter gold

nanoparticles were dispersed on the surface by a simple coating/evaporation process. Exposure of the gold-coated surface to silane gas at a pressure of 100 mTorr at 440°C for 30 min led to the formation of high density of SiNWs without any preferential orientation. Next, the gold nanoparticles were spotted on silicon oxide surface using a robot. The nanoparticles showed a high dispersion inside the spots. After reaction with SiH_4 at 440°C , SiNWs formation took place only on the edges of the spot and only few nanowires were observed inside the spot. Finally, gold nanodots (63 nm diameter) were deposited on the substrate using lithographic methods. When exposed to silane gas at 440°C , the silicon nanowires growth took place in all directions and in few cases, isolated SiNWs with an axis growth normal to the surface were observed. Increasing the temperature during the growth process led to an increase of the growth rate of the SiNWs. The fact that dispersed gold nanoparticles or patterned gold nanostructures on the surface did not lead to the formation of exclusively isolated SiNWs is in agreement with a motion of the metal catalyst at high temperature in the presence of the silane gas. Indeed, the electrostatic interactions between the oxide surface and the nanoparticles are not strong enough to hold the catalyst in its initial position.

Experimental details

Materials

All cleaning and etching reagents were clean-room grade. All chemicals were reagent grade or higher and were used as received unless otherwise specified. Monodisperse gold nanoparticles with an average diameter of 50 nm used in this study were purchased from Aldrich.

Sample preparation

Single side polished silicon $\langle 111 \rangle$ oriented *n*-type wafers (Siltronix) (phosphorus-doped, $R < 1$ ohm-cm resistivity) were first degreased in acetone and isopropanol, rinsed with Milli-Q water and then cleaned in 3:1 concentrated $\text{H}_2\text{SO}_4/30\% \text{H}_2\text{O}_2$ for 15 min at 80°C followed by copious rinsing with Milli-Q water.

(Caution: *piranha solution reacts violently with organic materials, it must be handled with extreme care, followed by copious rinsing with deionised water*)

Preparation of gold nanoparticles on Si/SiO₂ substrates

Monodisperse gold nanoparticles were purchased from Sigma. They display a mean particle size of 45–55 nm for the 50 nm.

Coating.

A drop of gold nanoparticles solution with different concentrations (dilution by a factor 2 or 10 in ethanol) was deposited on the oxidized silicon substrate. The hydrophilic surface was completely wetted by the drop and the solvent was evaporated at ambient atmosphere. The resulting surface was used without any further rinsing.

Spotting

Gold nanoparticles were spotted on the silicon substrate at different dilutions using a 4 piezo tips Perkin Elmer BioChip Arrayer (it is a non-contact microdispensing system designed specifically for pipetting sub-nanoliter volumes to dense arrays. Liquid volumes are precisely and accurately controlled by a patented piezoelectric tip technology that dispenses reproducible picoliter volume droplets to form dense arrays).

Patterning

Samples were prepared from an *n*-type Si(1 1 1) wafer. The samples were cleaned with acetone and isopropanol. They were then coated with polymethylmethacrylate (PMMA) photoresist and the disc pattern was transferred to the resist layer using a standard EBL technique. After development in methyl isobutyl ketone (MIBK) and rinsing in IPA, the samples were treated briefly with oxygen plasma to remove any resist residues from the exposed areas. The samples were then immediately transferred to a vacuum chamber where a 4 nm thick gold film was deposited via a thermal evaporation. Prior to gold deposition, the surface was treated with argon plasma to enhance metal adhesion on the silicon oxide surface. No titanium adhesion layer was used, because Ti [24] and TiSi₂ [25] are found to catalyze SiNWs growth in a different mechanism to the well-known VLS mechanism reported for gold. Moreover, Ti catalyst leads to the formation of tapered silicon nanowires under some processing conditions [24]. However, the resulting gold structures without any adhesion layer peel off under ultrasound cleaning during resist removing. Oxygen plasma treatment was thus preferred to ultrasound cleaning. The rough background in Fig. 3 results from the remaining resist on the surface after oxygen plasma treatment. The gold structures formed under these conditions have an average diameter of 63 nm. Some gold structures with an average size of 60 nm display island formation, while smaller gold dots (average size of 30 nm and below) are homogeneous. It is believed that the gold islands aggregate during SiNWs formation at high temperature to give a homogeneous gold structure.

Silicon nanowires synthesis

The samples coated with gold nanoparticles were transferred in a CVD reactor and were exposed to SiH₄ gaseous for 30 or 60 min at 100 mTorr (flow of SiH₄, $Q_{\text{SiH}_4} = 80$ Sccm) and heated at high temperatures (400–500°C) to produce a dense array of nanowires. The resulting surfaces were characterized using scanning electron microscopy (SEM).

Scanning electron microscopy

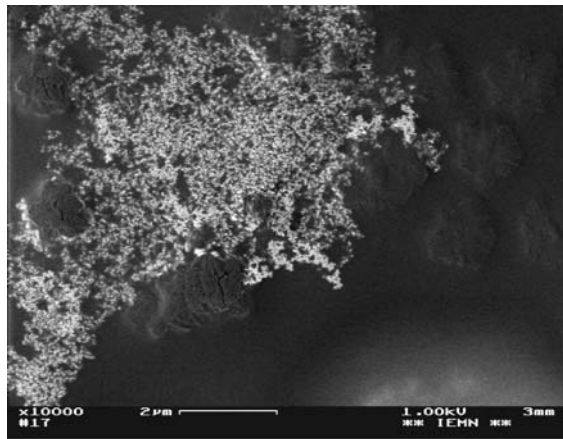
Electron microscopy was carried out with a LEO 982 field-emission scanning electron microscope (SEM) with an image resolution of 2.1 nm at 1 KV and 1.5 nm at 15 KV at the analytical working distance.

Results and discussion

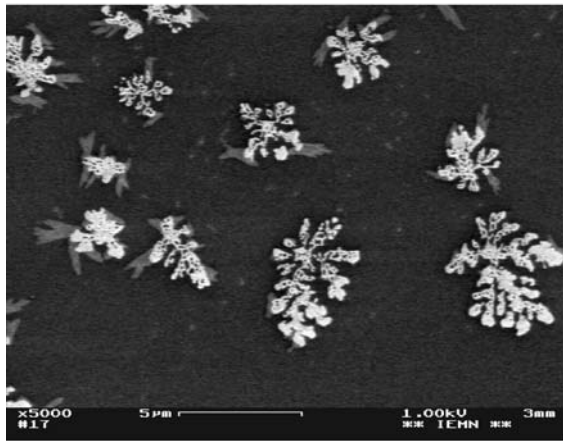
Studies of gold nanoparticles dispersion on oxidized silicon surfaces

In this study, we used Au nanoparticles as catalysts as it does not form silicide compared to titanium [24, 25] and iron [26]. Moreover, Au/Si eutectic temperature is relatively low (363°C) compared to other catalysts. At temperatures higher than 363°C, Au and Si form a liquid alloy, which dissolves some of the silicon from the gas SiH₄ stream. When the liquid metal reaches saturation, silicon crystals start precipitating out and initiate the growth of the nanowire against the substrate. As the crystal grows, it lifts the liquid catalyst up and a silicon nanowire forms. The diameter and the length of the SiNW are controlled by the nanoparticle diameter and the reaction time, respectively.

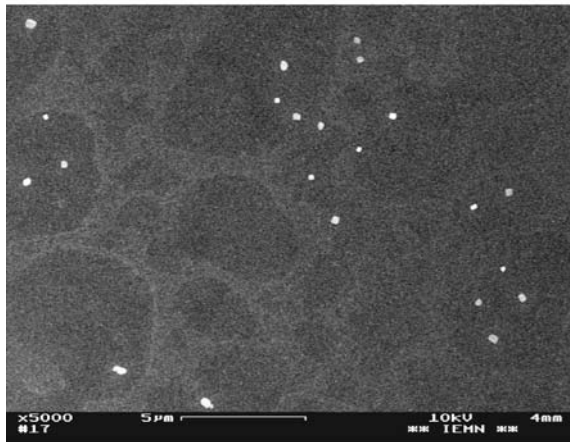
We have first examined the gold nanoparticles distribution on silicon oxide surfaces obtained by simple coating/evaporation of the surface with the nanoparticles at different concentrations. Figure 1(a) displays a SEM image of a clean surface of Si/SiO₂ covered with 50 nm diameter gold nanoparticles aqueous solution (as received without any further dilution) after solvent evaporation. The SEM image clearly shows metal aggregation on the surface (Fig. 1(a)). Dilution of the parent solution (by a factor 2 in ethanol) led to the formation of dendrite-like structures in a reproducible fashion on the surface after slow evaporation of the solvent at room temperature (Fig. 1(b)). Further dilution of the nanoparticles solution had a pronounced effect on the gold nanoparticles distribution on the surface. Figure 1(c) exhibits a SEM image of an oxide surface covered with 50 nm diameter gold nanoparticles aqueous solution diluted by a factor 10 in ethanol, after evaporation of the solvent. A very nice dispersion of the particles on the surface was obtained.



(a)



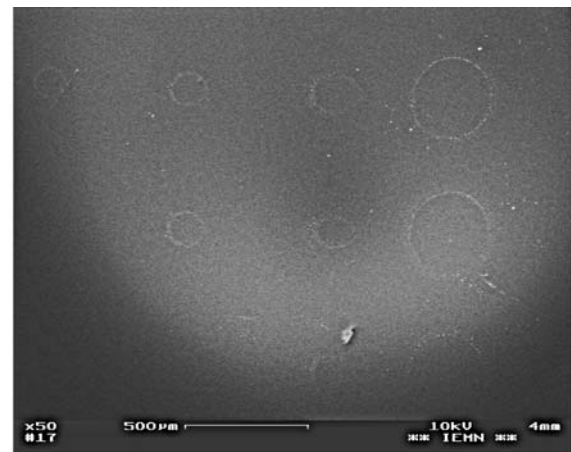
(b)



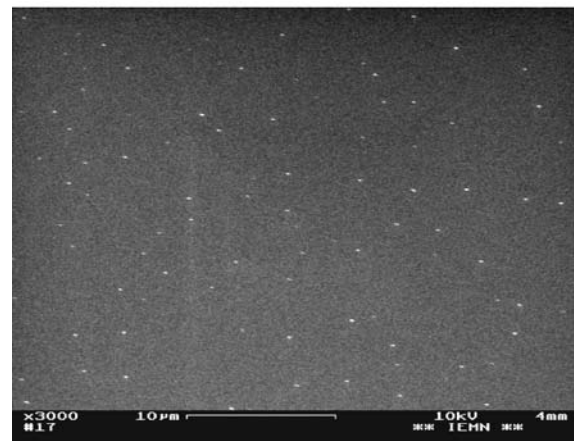
(c)

Fig. 1 SEM images of silicon (1 1 1) surfaces coated with gold nanoparticles at different concentrations: as received without any dilution (a); diluted in ethanol by a factor 2 (b); diluted in ethanol by a factor 10 (c)

In the next stage, we have used a robot to spot gold nanoparticles aqueous solution diluted by a factor 10 in ethanol on oxidized silicon surfaces. Figure 2(a) corresponds to a SEM image of the resulting spots with different sizes. The edge of the spots appears as bright circles compared to



(a)



(b)

Fig. 2 SEM images of (a): the different spots of gold nanoparticles (diluted in ethanol by a factor 10) on oxidized silicon surfaces, and (b): taken inside the spot

the rest of the spot, which looks smooth and homogeneous. This is consistent with a concentration gradient of gold nanoparticles at the spot edges. The phenomenon may be explained by the migration of the gold nanoparticles from the center to the edge of the spot during solvent evaporation process. This effect known as “doughnut effect” was reported for c-DNA microarrays and common with hydrophilic surfaces [27]. The difference in size of the spots is due to the number of nano droplets dispensed by the tip on the same spot. Detailed analysis by SEM shows a good dispersion of the gold nanoparticles inside the spots (Fig. 2(b)).

It is apparent from the VLS nanowire growth mechanism that the positions of nanowires on the surface can be controlled by the initial positions of Au clusters or thin films. Various lithographical techniques including, for example, soft lithography, e-beam, and photolithography, can be used to create patterns of the Au thin film for the subsequent semiconductor nanowire growth. *E*-beam lithography was finally adopted to create nano patterns of gold on oxidized silicon surface. Gold structures with 63 nm

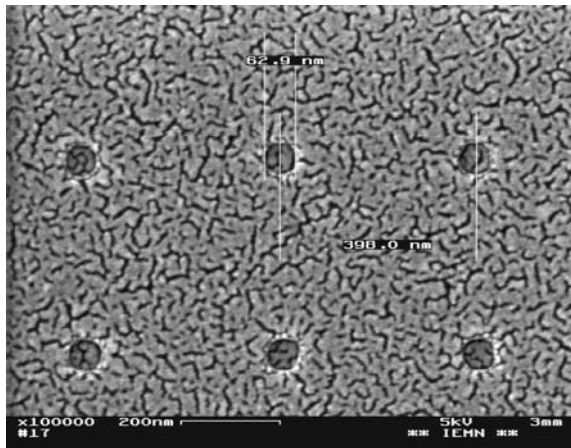


Fig. 3 SEM image the patterned gold nanodots prepared by e-beam lithography after lift off. The gold nanodots have a mean diameter of 63 nm and separated by 398 nm

average diameter separated by 400 nm (distance center to center) were deposited on the surface in a controlled fashion as shown by SEM (Fig. 3).

Silicon nanowires growth

Before proceeding to nanowire growth, we have tested the thermal behavior of the oxidized silicon surfaces coated with gold nanoparticles (from Fig. 1(c)). Thermal treatment at temperatures ranging from 400 to 600°C did not show any shape or size evolution in the absence of silane gas. Exposure of the same surface to silane gas at a pressure of 100 mTorr at 440°C for 30 min (Q : 80 sccm) led to silicon nanowires growth (Fig. 4). The obtained nanowires are terminated by gold seeds according to the VLS growth mechanism. However, the resulting nanowires display a large size distribution and in few cases exhibit growth defects, such as bends and kinks. These defects result from the low stability of the

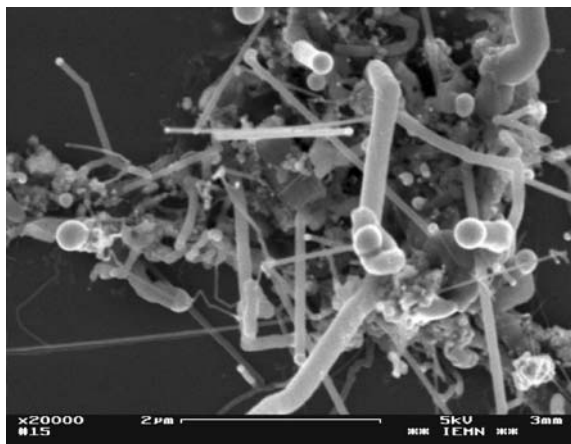
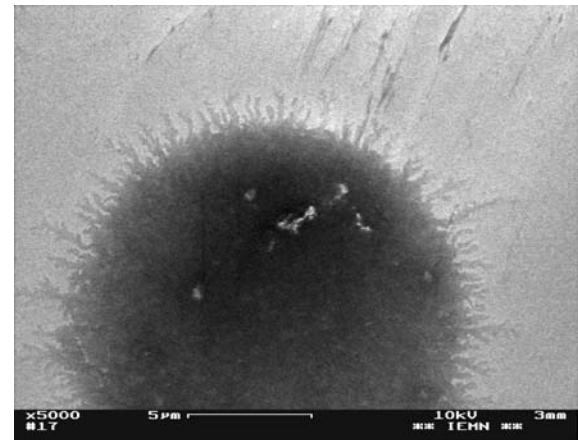


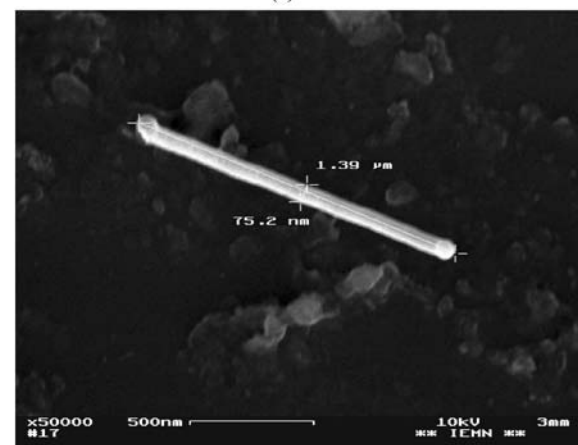
Fig. 4 SEM image of silicon nanowires grown on silicon oxide surfaces coated with 50 nm diameter gold nanoparticles (from Fig. 1(c)) prepared at a silane pressure of 100 mTorr at 440°C for 30 min

Au/Si liquid droplet with the growing Si nanowire interface once growth is nucleated. Moreover, the SEM image (Fig. 4) shows that the SiNWs are concentrated in a very small area and not isolated on the surface in contrast to the initial gold nanoparticles distribution. Since the diameter of the nanowire is determined by the size of the droplet alloy, which is in turn determined by the original cluster size, we do believe that during the growth process, nanoparticles aggregation occurred.

In the next experiment, we have prepared SiNWs on oxidized silicon surfaces on which 50 nm diameter gold nanoparticles (diluted by a factor 10 in ethanol) were previously spotted using a robot. Under the same growth conditions as previously, the silicon nanowire growth took place exclusively at the edges of the spots (Fig. 5(a)). A close SEM investigation of the central parts of the spot showed some isolated SiNWs with an average diameter of 50 nm (Fig. 5(b)). The result was assigned to the migration of the gold nanoparticles from the center to the edge of the spot



(a)



(b)

Fig. 5 SEM images of silicon nanowires prepared at SiH_4 pressure of 100 mTorr at 440°C for 30 min ($Q_{\text{SiH}_4} = 80$ sccm) on Si/SiO₂ surfaces catalyzed by spotted gold nanoparticles. The SiNWs were mainly observed on the spot edges (a) while only few nanowires were formed in the central parts of the spots (b)

during solvent evaporation process. This phenomenon happened only when the surface was subjected to the silane gas stream at high temperature. Indeed, the SEM analysis of the surface just after nanoparticles deposition showed a homogeneous dispersion of the catalyst on the whole surface of the spot (Fig. 2(b)) and a higher concentration of gold nanoparticles at the edges (Fig. 2(a)). The SiNW growth followed the same trend of the catalyst concentration at the spot edges.

Finally, SiNWs were grown on lithographically patterned surfaces. The gold catalyst deposited by this technique has an average diameter of 63 nm and separated by 400 nm. The SiNWs growth was accomplished under the same experimental conditions as previously (gas pressure: 100 mTorr at 440°C for 30 min (Q: 80 sccm)). SEM analysis has illustrated the formation of dense nanowires on certain regions of the surface (Fig. 6), while isolated nanowires have also been seen in other regions. The isolated nanowires display an average diameter of 53 nm and are 1.8 μm long (Fig. 7(a)). The isolated nanowires grow in a preferential direction normal to the silicon surface. The presence of isolated nanowires located only in the area where the gold was deposited along with regions with a high density of nanowires is not clear. This result may account for the thermal aggregation of the gold nanostructures in the presence of silicon gas during the VLS process.

We had further investigated the influence of the time and the temperature on the silicon nanowire growth. In a first approach, the temperature and the gas pressure were kept constant and the reaction time was varied from 30 to 60 min. Figure 7(b) displays the SEM image of isolated nanowire grown at a silane pressure of 100 mTorr at 440°C for 60 min. The SiNWs growth took place in a similar way as previously. The surface was composed of regions with a high density of nanowires and isolated ones. The isolated nanowires exhibit this time an average diameter of 68 nm and a length of

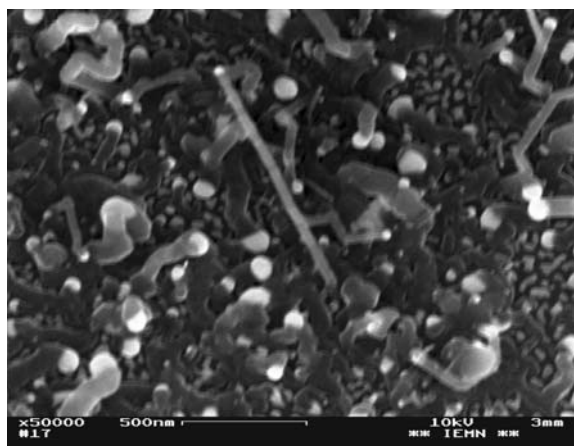
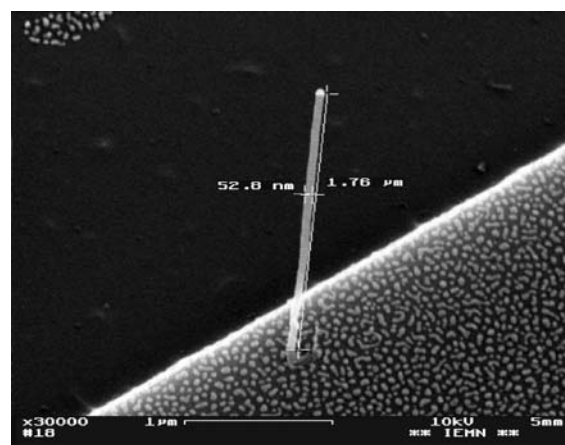
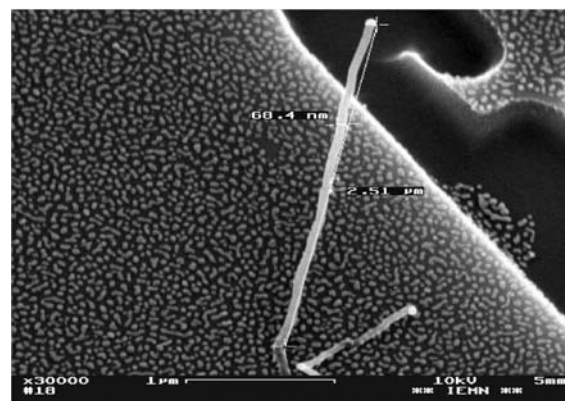


Fig. 6 SEM image of SiNWs synthesized on an e-beam patterned surface at SiH_4 pressure of 100 mTorr at 440°C for 30 min



(a)



(b)

Fig. 7 SEM images of isolated silicon nanowires formed on an e-beam patterned surface at SiH_4 pressure of 100 mTorr at 440°C for (a) 30 min and (b) 60 min

2.5 μm . The length of the nanowire increased by a factor 1.4 compared to the one obtained after 30 min reaction (1.8 μm) (Fig. 7(a)). The SiNWs length depend on the reaction time as reported in the literature [28]. Scanning transmission electron

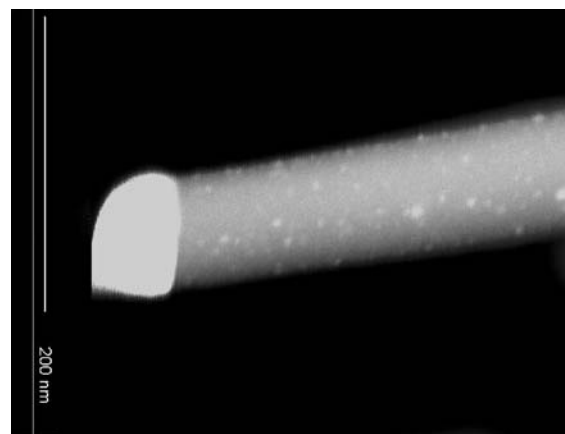


Fig. 8 Scanning Transmission Electron Microscopy (STEM) of isolated silicon nanowires formed on an e-beam patterned surface at SiH_4 pressure of 100 mTorr at 440°C

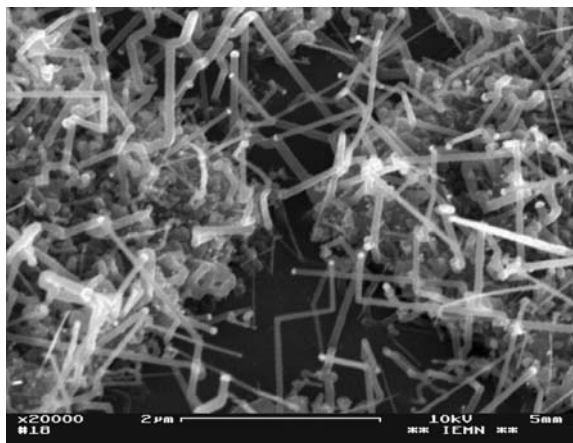


Fig. 9 SEM image of SiNWs obtained on an e-beam patterned surface at SiH₄ pressure of 100 mTorr at 500°C for 30 min

microscopy (STEM) analysis of the resulting nanowires deposited on a TEM grid shows SiNWs with an average diameter around 60 nm, in agreement with the size of the starting gold catalyst (Fig. 8).

Next, the temperature was increased up to 500°C while keeping the reaction time and the gas pressure constant (100 m Torr, 30 min). SEM analysis shows SiNWs with features comparable to the ones obtained at 440°C with more kinks and bends (Fig. 9).

Conclusions

In summary, we have synthesized silicon nanowires on Si/SiO₂ with an average diameter of 50 nm and few microns long using SiH₄ as the silicon source and gold as the mediating solvent in a VLS process. Three different techniques have been used for gold deposition. When the nanoparticles were simply dispersed or spotted on the surface, a high density of silicon nanowire formation without any preferential axis growth was observed. However, isolated silicon nanowires with an orientation normal to the surface were prepared when the gold catalyst was patterned on the surface using e-beam lithography. The diameter of the silicon nanowires is controlled by gold cluster diameter and the length by the reaction time. Future work will focus on the synthesis of isolated SiNWs on the surface under controlled conditions in a predictive way and the study of their electrical and optical properties. Further surface characterization of the SiNWs to evaluate their elemental composition and crystallinity under progress. Improvement of the gold deposition and the size distribution using MESA patterning process is under investigation in the laboratory. Surface chemistry of the nanowires will have a big impact on their electrical characteristics. The control of the interfacial properties of the nanowire/thin oxide

passivating layer will play a key role in the efficiency of the devices based on SiNWs, under operation.

Acknowledgments The authors thank Dr. Oleg Melnyk and Dr. Yannick Coffinier for helping with the gold nanoparticle spotting. The Centre National de la Recherche Scientifique (CNRS) and the Nord-Pas-de Calais region are gratefully acknowledged for financial support.

The Deutsch-Französische Hochschule foundation, the University of Erlangen-Nuremberg, the University of Provence, the CNRS, Metrohm, Autolab and Raith are also acknowledged for their financial support of the “First German-French Summer School on Electrochemistry and Nanotechnology”.

References

1. Y. Cui, Z. Zhong, D. Wang, W.U. Wang, and C.M. Lieber, *Nano Lett.*, **3**, 149 (2003).
2. Y. Cui and C.M. Lieber, *Science*, **291**, 851 (2001).
3. J.-W. Chung, J.-Y. Yu, and J.R. Heath, *Appl. Phys. Lett.*, **76**, 2068 (2000).
4. Y. Cui, Q. Wei, H. Park, and C.M. Lieber, *Science*, **293**, 1289 (2001).
5. J.-in Hahm and C.M. Lieber, *Nano Lett.*, **4**, 51 (2004).
6. M.H. Huang, S. Mao, H. Feick, H. Yan, Y. Wu, H. Kind, E. Weber, R. Russo, and P. Yang, *Science*, **292**, 1897 (2001).
7. M.C. McAlpine, R.S. Friedman, S. Jin, K.-H. Lin, W.U. Wang, and C.M. Lieber, *Nano Lett.*, **3**, 1531 (2003).
8. Q. Peng, Z. Huang, and J. Zhu, *Adv. Mater.*, **16**, 73 (2004).
9. M. Morales and C.M. Lieber, *Science*, **279**, 208 (1998).
10. N. Wang, Y.H. Tang, Y.F. Zhang, D.P. Yu, C.S. Lee, I. Bello, and S.T. Lee, *Chem. Phys. Lett.*, **283**, 368 (1998).
11. Y.F. Zhang, Y.H. Tang, N. Wang, D.P. Yu, C.S. Lee, I. Bello, and S.T. Lee, *Appl. Phys. Lett.*, **72**, 1835 (1998).
12. N. Wang, Y.H. Tang, Y.F. Zhang, C.S. Lee, I. Bello, and S.T. Lee, *Chem. Phys. Lett.*, **299**, 237 (1999).
13. R.S. Wagner and W.C. Ellis, *Appl. Phys. Lett.*, **4**, 889 (1964).
14. R.S. Wagner, in *Whisker Technology*, edited by (A.P. Levitt, Wiley, New York, 1970) p. 47.
15. J. Westwater, D.P. Gosain, S. Tomiya, S. Usui, and H. Ruda, *J. Vac. Sci. Technol. B*, **15**, 554 (1997).
16. J. Westwater, D.P. Gosain, and S. Usui, *Jpn. J. Appl. Phys.*, **36**, 6204 (1997).
17. Y. Cui, X. Duan, J. Hu, and C.M. Lieber, *J. Phys. Chem. B*, **104**, 5213 (2000).
18. Y. Cui, L.J. Lauhon, M.S. Gudiksen, J. Wang, and C.M. Lieber, *Appl. Phys. Lett.*, **78**, 2214 (2001).
19. Y. Wu, Y. Cui, L. Huynh, C.J. Barrelet, D.C. Bell, and C.M. Lieber, *Nano Lett.*, **4**, 433 (2004).
20. Y. Wu and P. Yang, *J. Am. Chem. Soc.*, **123**, 3165 (2001).
21. J.D. Holmes, K.P. Johnston, R.C. Doty, and B.A. Korgel, *Science*, **287**, 1471 (2000).
22. T. Hanrath and B.A. Korgel, *Adv. Mater.*, **15**, 437 (2003).
23. X. Lu, T. Hanrath, K.P. Johnston, and B.A. Korgel, *Nano Lett.*, **3**, 93 (2003).
24. S. Sharma, T.I. Kamins, and R. Stanley Williams, *J. Cryst. Growth*, **267**, 613–618 (2004).
25. T.I. Kamins, R. Stanley Williams, Y. Chen, Y.-L. Chang, and Y.A. Chang, *Appl. Phys. Lett.*, **76**, 562 (2000).
26. Q. Gu, H. Dang, J. Cao, J. Zhao, and S. Fan, *Appl. Phys. Lett.*, **76**, 3020 (2000).
27. R. Blossey and A. Bosio, *Langmuir*, **18**, 2952 (2002).
28. J.W. Dailey, J. Taraci, T. Clement, D.J. Smith, J. Drucker, and S.T. Picraux, *J. Appl. Phys.*, **96**, 7556 (2004).